Eur. Phys. J. D **20**, 269–274 (2002)
DOI: 10.1140/epjd/e2002-00125-0

THE EUROPEAN PHYSICAL JOURNAL D

Advanced simulations of spectroscopic signatures of charge exchange in laser-produced plasmas

E. Leboucher-Dalimier[1,a], E. Oks[2], E. Dufour[1], P. Angelo[1], P. Sauvan[3], R. Schott[1], and A. Poquerusse[1]

[1] Physique Atomique dans les Plasmas Denses[b], CNRS-École Polytechnique-CEA-Université Paris-VI, Case 128, 4 place Jussieu, 75252 Paris Cedex 05, France
[2] Physics Department, 206 Allison Lab., Auburn University, Auburn AL 36849, USA
[3] Instituto de Fusión Nuclear, E.T.S. de Ingenieros Industriales U.P.M., Jose Gutierrez Abascal, 2 – 28006 Madrid, Spain

Received 25 March 2002
Published online 19 July 2002 –

Abstract. We present an advanced theory of charge-exchange-caused dips (also called X-dips) in spectral lines from laser-produced plasmas. We compare predictions of this advanced theory with our previously published experimental results where, in the process of a laser irradiation of targets made out of aluminum carbide, we observed two X-dips in the L_γ line of Al XIII perturbed by fully stripped carbon. We show that our advanced theory is in excellent agreement with our experimental results. From the practical point of view, our results open up a way to experimentally produce not-yet-available fundamental data on charge exchange between multicharged ions, virtually inaccessible by other experimental methods. From the theoretical viewpoint, the results are important because the X-dips are the only one signature of charge exchange in profiles of spectral lines emitted by plasmas and they are the only one quasimolecular phenomenon that could be observed at relatively "low" densities of laser-produced plasmas.

PACS. 52.70.Kz Optical (ultraviolet, visible, infrared) measurements – 32.70.Jz Line shapes, widths, and shifts

1 Introduction

Charge Exchange (CE) is a fundamental process of a great practical importance (see, *e.g.*, book [1]). For example, in magnetic fusion devices it occurs in the divertor region as well as during the injection of neutral beams or solid pellets. Specifically, CE between multicharged impurity ions and hydrogen (or deuterium, or tritium) atoms in tokamaks provides a nonlinear coupling of kinetics of impurities and neutrals, thus affecting the feasibility of controlled fusion (since multicharged ions produce considerably more radiative losses per unit particle than singly charged ions of the nuclear fuel components) – see, *e.g.*, [2,3] and references therein. CE in tokamaks is also used for diagnostics – to measure the density of impurity ions while injecting a neutral beam in the plasma (see, *e.g.*, [1]). Second, CE was proposed as one of the most effective mechanisms for population inversion in the soft X-ray and VUV ranges [1,4–7]. In this scheme, an inversion is created by a selective quasi-resonant population of excited ionic levels due to the interaction of a multicharged ionic beam with cold gaseous or low-charged plasma targets. Particularly, such beams or jets could be generated due to instabilities in axial discharges [8–11]. Third, CE involving multicharged ions is also a controlling factor in ion storage devices (see, *e.g.*, [12]). Fourth, CE plays an important role in astrophysics, *e.g.*, for the solar plasma and for determining the physical state of planetary nebulae [1].

In addition, there is a recent theoretical development on CE that yielded counterintuitive results. Indeed, the paradigm was that CE is described in terms of electron tunneling between two potential wells and is therefore an inherently quantum phenomenon (see, *e.g.*, a textbook [13], p. 286). However, in recent papers [14,15] it was shown that CE can also be described in a purely classical (not even semiclassical) formalism starting from first principles.

In view of the practical and theoretical significance of CE, it would be important to find new experimental approaches for measuring CE cross-sections – especially, for multicharged ions. Indeed, experimental CE cross-sections relevant to magnetic fusion measured by various techniques (*e.g.*, by a merged-beam technique [16]) are known only for situations where one of the colliding partners has a nuclear charge $Z \leq 2$ (see, *e.g.*, [17,18]). There is virtually no fully-developed experimental methods for measuring cross-sections of CE where both colliding partners have charges Z, $Z' \gg 1$. For this practically important situation, seemingly the best existing experimental

[a] e-mail: lebda@moka.ccr.jussieu.fr
[b] LULI Unité mixte No. 7605

approaches in their present form do not allow to measure CE cross-sections yet, but only to observe some X-ray signatures of CE in K- or L-shell emission (see, *e.g.*, [12] and references therein).

We proposed an alternative experimental approach based on CE-caused dips (also called X-dips) in spectral lines emitted by plasmas. The X-dips are a relatively new phenomenon. It was first observed in the profile of the neutral hydrogen line H_α emitted from a helium plasma of the gas-liner pinch [19]. That paper [19] also gave a sketch of the underlying theory.

Subsequent works [20,21] presented a more sophisticated theory of the X-dip phenomenon. These theoretical works [20,21] focused at the possibility of observing the X-dips in spectral lines of *multicharged* ions in laser-produced plasmas. The reason for this focus is that the X-dips phenomenon can open up an alternative, new way to experimentally obtain data on CE between multicharged ions. For most pairs of multicharged ions this might be the only one way to obtain such an experimental information of a fundamental importance. The theoretical papers [20,21] provided a list of pairs of multicharged ions, which were the most favorable candidates for observing the X-dips in laser-produced plasmas. This list contains particular spectral lines of some hydrogen-like ions of a nuclear charge Z perturbed by some particular fully-stripped ions of a nuclear charge $Z' \neq Z$.

In our previous experimental paper [22] we presented the first experimental observation of the X-dips in spectral lines of multicharged ions in laser-produced plasmas. Specifically, in the process of a laser irradiation of targets made out of aluminum carbide, we observed two X-dips in the L_γ line of Al XIII perturbed by fully stripped carbon. These experimental results were compared in [22] with predictions of the analytical theory [20,21] that was asymptotic – valid for relatively large internuclear distances R.

In the present paper we report simulations that significantly advance the underlying theory. First, in these simulations we do not use the assumption that values of R are relatively large. Second, we take into account the shielding by electrons, which results in a polarization shift of energy levels. Finally, we compare predictions of this advanced theory with our experimental results.

2 Asymptotic analytical theory of the X-dip phenomenon

An analytical theory of the X-dip phenomenon was presented in [20,21]. In this section we give some brief excerpts from [20,21] that are necessary for presenting a new advance in the underlying theory in the next section.

We consider electron terms in the field of two stationary Coulomb centers of charges Z and Z' separated by a distance R. Specifically, we consider a term of a principal quantum number n, which asymptotically (at $R \to \infty$) is a radiator's term (hereafter, Z-term), and a term of a principal quantum number n', which asymptotically is a perturber's term (hereafter, Z'-term). We are interested in the situation where in the vicinity of R_0 there occurs an avoided crossing of the term n with the term n'.

We deal with a radiative transition between the Z-term n and some lower Z-term n_0 resulting in a Stark component of the corresponding hydrogenlike spectral line. We use atomic units and therefore employ the same notation $f(R)$ for both the transition energy and the transition frequency; R is the distance between the radiator and the perturbing atom or ion. We focus at a vicinity of the crossing distance R_0 corresponding to a small part of the component profile around $\Delta\omega_0 = f(R_0)$.

For a minority of radiators for which the distance R is close to R_0, due to the avoided crossing of the terms, CE appears as an *additional channel for decay* of the excited state of the Z ion. Therefore the lifetime of the excited state is shorted and the collisional width *suddenly* increases. This means that these radiators emit a broader collisional profile (compared to the others), which is consequently less intense in its central part and more intense in its wings. Thus at the frequency $\Delta\omega[f(R_0)]$ the intensity of the resultant line profile becomes smaller than it would be if the avoided crossing was absent. As a result, a dip (called "X-dip") might appear in the line profile.

The analytical theory developed in [20,21] was valid asymptotically. In other words, it was assumed in [20,21] that a CE-caused avoided crossing occurs at a relatively large distance:

$$R \gg \max(n^2/Z, n'^2/Z'). \tag{1}$$

There are upper and lower limits that determine the range of electron densities, where the X-dips can be observed [20,21]. Both the lower limit and one out of two competing values of the upper limit physically come from the requirement that the crossing distance R_0 should not differ too much from the most probable internuclear distance. Another upper limit physically comes from the condition that the dynamical Stark broadening by electrons and ions of the plasma should not be so large as to wash out the dip.

This theory was applied in [20,21] for selecting prospective ZeZ'-systems for observations of X-dips in laser-produced high-density plasmas of multicharged ions. One of the prospective candidates was the L_γ line of Al XIII ($Z = 13$) perturbed by fully-stripped C ($Z' = 6$). Avoided crossings of some of the $Z = 13$ terms of $n = 4$ with some of the $Z' = 6$ terms of $n' = 2$ occur in a vicinity of $R_0 \approx 8$ au. This distance is about 6.5 times greater than the size n^2/Z of the largest out of the two separate states (Z, n) and (Z', n'). More specifically, the avoided crossings can be described using electric quantum numbers $q \equiv n_1 - n_2$ and $q' \equiv n'_1 - n'_2$ as follows. The avoided crossing of the $(Z, 4)$-term of $q = -2$ with the $(Z', 2)$-term of $q' = 0$ should translate into an X-dip located at $\Delta\lambda \approx 6.7$ mÅ (*i.e.*, on the red side). In addition, the avoided crossing of the $(Z, 4)$-term of $q = -3$ with the $(Z', 2)$-term of $q' = -1$ should translate into an X-dip located at $\Delta\lambda \approx 9.6$ mÅ (*i.e.*, on the red side). The range of densities where these two X-dips could be

observed (for $T \sim 400$ eV) is: $N_{\rm e}^{\rm upper} \approx 1 \times 10^{22}$ cm^{-3}, $N_{\rm e}^{\rm lower} \approx 2 \times 10^{20}$ cm^{-3}.

3 Advanced simulations of the X-dip phenomenon

The above theoretical results were obtained analytically using the assumption (1). Therefore it would be important to improve the accuracy of these asymptotic results (valid for relatively large R) by numerical computations that would not employ the assumption (1). In addition, for relatively large R, the shielding by electrons (resulting in a polarization shift of energy levels) should be also taken into account.

We achieved both these goals by using the code IDEFIX. This code is based on the following dicenter model. Two ionic centers (such as Al^{13+} and C^{6+} in our particular case), which are the nearest neighbors sharing one bound electron, are immersed in a non-uniform gas of free electrons within a radiating cell [23–27].

For each avoided crossing, we performed two different runs of the IDEFIX. In the first run, the energy levels were calculated by numerical diagonalization of the corresponding Hamiltonian, but without taking into account the electronic shielding (*i.e.*, formally for $N_{\rm e} = 0$). In the second run, the electronic shielding was incorporated in the process of diagonalizing the Hamiltonian in a self-consistent fashion. Specifically, the second run was done for $N_{\rm e} = 10^{22}$ cm^{-3}, *i.e.*, for the upper limit of the density range where the two X-dips are expected to be observed. The results are as follows.

For the pair of the $(Z, 4)$-term of $q = -2$ and the $(Z', 2)$-term of $q' = 0$, at $N_{\rm e} = 0$ the avoided crossing occurs at $R = 8.00$ au and at the energy $E_1 = -6.12$ au (see Fig. 1). At $R = 8.00$ au, the energy of the ground level of Al XIII is $E_0 = -85.25$ au. Thus the absolute position of the crossing should be 79.13 au in the energy scale or 5.758 Å in the wavelength scale. Since for the center of the L_γ line of Al XIII (*i.e.*, for its unperturbed position) the IDEFIX yields 5.751 Å, the relative position of the expected X-dip becomes $\Delta\lambda = 7$ mÅ. This value is close to the corresponding asymptotic result of $\Delta\lambda \approx 6.7$ mÅ given above.

At $N_{\rm e} = 10^{22}$ cm^{-3}, the allowance for the electronic shielding shifts the crossing of the same pair of terms to $R = 7.43$ au and $E_1 = -4.32$ au (see Fig. 2). However, with the allowance for the electronic shielding, the energy of the ground level of Al XIII at $R = 7.43$ au is now $E_0 = -83.45$ au. Thus the absolute position of the crossing at $N_{\rm e} = 10^{22}$ cm^{-3} remains the same as it was at $N_{\rm e} = 0$: 79.13 au in the energy scale or 5.758 Å in the wavelength scale. At $N_{\rm e} = 10^{22}$ cm^{-3}, for the center of the L_γ line of Al XIII the IDEFIX yields 5.752 Å. Therefore, with the allowance for the electronic shielding the relative position of the expected X-dip becomes $\Delta\lambda = 6$ mÅ (on the red side).

Similarly, for the pair of the $(Z, 4)$-term of $q = -3$ and the $(Z', 2)$-term of $q' = -1$, at $N_{\rm e} = 0$ the avoided crossing occurs at $R = 8.50$ au and at the energy $E_1 = -6.125$ au. At $R = 8.50$ au, the energy of the ground level of Al XIII is $E_0 = -85.21$ au. Thus the absolute position of the crossing should be 79.08 au in the energy scale or 5.762 Å in the wavelength scale. Since for the center of the L_γ line of Al XIII (*i.e.*, for its unperturbed position) the IDEFIX yields 5.751 Å, the relative position of the second expected X-dip becomes $\Delta\lambda = 11$ mÅ. This value is more precise than the corresponding asymptotic result of $\Delta\lambda \approx 9.6$ mÅ given above.

At $N_{\rm e} = 10^{22}$ cm^{-3}, the allowance for the electronic shielding shifts the crossing of the latter pair of terms

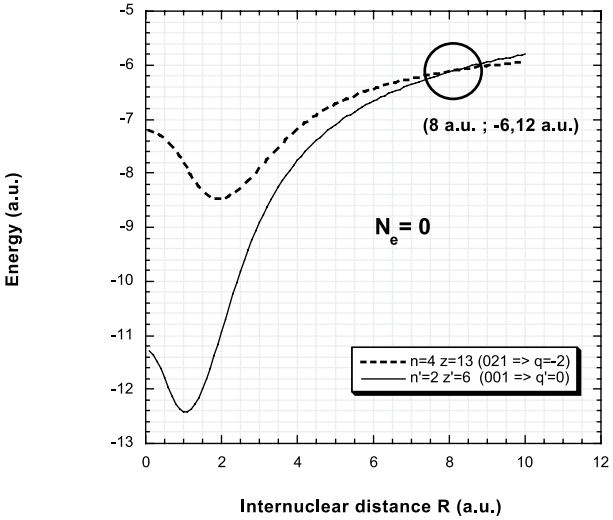

Fig. 1. Crossing of the term $\{n = 4, q = -2\}$ of Al XIII perturbed by C^{6+} (dashed line) with the term $\{n' = 2, q' = 0\}$ of C VI perturbed by Al^{13+} (solid line) *without* the allowance for the electronic shielding, *i.e.*, formally for the electron density $N_{\rm e} = 0$. The avoidance of the crossing is not shown.

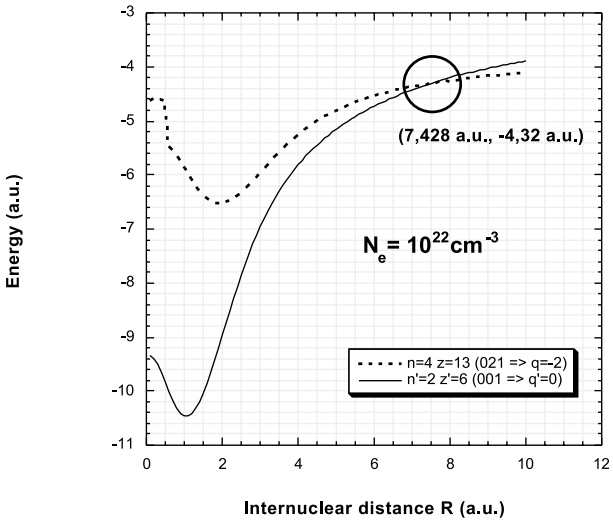

Fig. 2. Crossing of the term $\{n = 4, q = -2\}$ of Al XIII perturbed by C^{6+} (dashed line) with the term $\{n' = 2, q' = 0\}$ of C VI perturbed by Al^{13+} (solid line) *with* the allowance for the electronic shielding for the electron density $N_{\rm e} = 10^{22}$ cm^{-3}. The avoidance of the crossing is not shown.

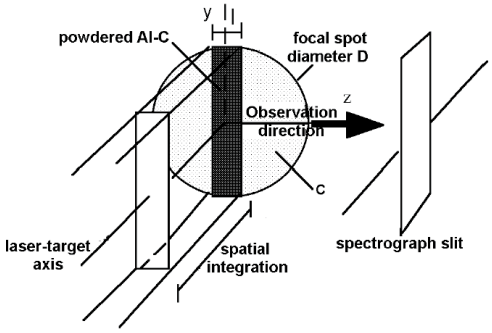

Fig. 3. Experimental set up, including the design of the structured target. The aluminum carbide plasma is confined in a carbon plasma in the direction of the observation, thus allowing the control of the re-absorption. The Al_4C_3 strips, centered on the laser beam, are well suited for the optimization of the emission. The spectrograph slit ensures a spatial resolution along the laser-target axis.

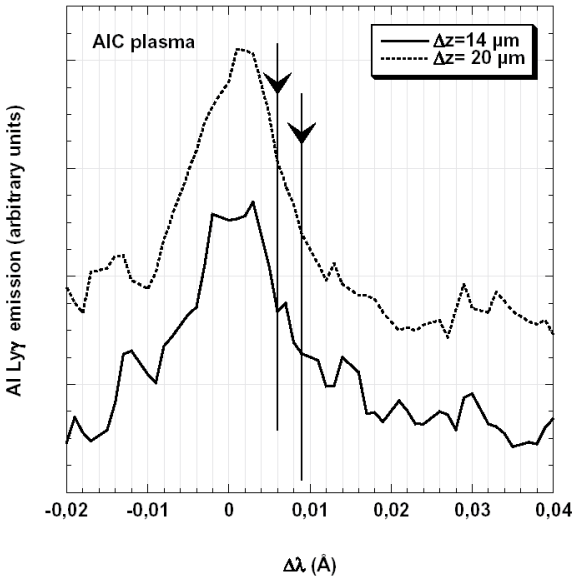

Fig. 4. Experimental profiles of the Ly_γ line of Al XIII emitted from an aluminum carbide plasma for two spatially integrated slices Δz, the thickness of which is counted from the bottom of the crater toward the corona plasma. For $\Delta z = 14$ μm corresponding to the densities 10^{20}–10^{22} cm^{-3}, the profiles exhibit two pronounced dips in the *near* red wing. For $\Delta z = 20$ μm, only discontinuities of the slope of the line profile in the *near* red wing are still visible as remnants of the X-dips. In the latter case, the average density for the selected plasma slice is getting too low for observing the X-dips, the densest part of the plasma being hidden by the slit (15 μm). The observed dips, being located in the *near* wing, correspond to the part of the line profile where the signal-to-noise ratio is still reasonable. Besides, they are reproducible in all spectra observed for different Δz. These two features distinguish the observed dips from the jitter in the far wings. The latter corresponds to the experimental noise and its spectral positions are not reproducible in spectra observed for different Δz.

to $R = 7.93$ au and $E_1 = -4.32$ au. Further, with the allowance for the electronic shielding, the energy of the ground level of Al XIII at $R = 7.93$ au is now $E_0 = -83.41$ au. Thus for the absolute position of the crossing at $N_e = 10^{22}$ cm^{-3} we obtained: 79.09 au in the energy scale or 5.761 Å in the wavelength scale. At $N_e = 10^{22}$ cm^{-3}, for the center of the L_γ line of Al XIII the IDEFIX yields 5.752 Å. Therefore, with the allowance for the electronic shielding the relative position of the expected X-dip becomes $\Delta\lambda = 9$ mÅ (on the red side).

We would like to emphasize two points. First, without the allowance for the electronic shielding, our simulations yield X-dip positions shifted by up to 14% compared to the asymptotic analytical calculations. Second, the allowance for the electronic shielding shifts both the upper and lower levels involved in the radiative transition much more than their difference (and thus the transition frequency), as should be expected for relatively large R. The shift of the transition frequency (and therefore, of the X-dip positions) due to the electronic shielding is up to 21%, but in the direction opposite to the shift mentioned in the first point.

4 Experiment

In this section we briefly re-iterate our experimental discovery of the X-dips in the L_γ line of Al XIII perturbed by fully stripped carbon in a laser-produced plasma (published in [22]) and then compare these experimental results with our advanced theory. The experiment was performed at the nanosecond laser facility at the LULI, France. When a high intensity (4×10^{14} W/cm^2) 4ω laser beam in a pulse of 500 ps is focused onto a massive target, the electron density and temperature can reach extreme values such as 10^{23} cm^{-3} and 300 eV respectively in the first five microns of the plasma inside the crater. The density and the temperature gradients in the adjacent layer of 10–15 microns can be easily diagnosed by emission spectroscopy.

The experimental setup designed to optimize both the generation and the diagnostics of the X-dips in the Ly_γ line of Al XIII perturbed by fully-stripped carbon is shown in Figure 3.

The targets were structured: powdered aluminum carbide (Al_4C_3) strips are inserted in a carbon substrate. For each target, the Al_4C_3 strip was placed through the center of the focal spot (Ø = 80 μm). They are well suited for the optimization of the emission intensity and for the control of both the transverse inhomogeneities and the re-absorption. It turned out that, for the density domain 10^{20}–10^{22} cm^{-3} required for observing the X-dips in the Ly_γ line of Al XIII, thin strips of the thickness 20 μm well served the above purpose [22,23].

A diagnostic of an ultra-high spatial and spectral resolution recorded spectra emerging from progressively thicker slices of plasma, perpendicularly to the laser beam, with the help of the 15 μm slit. This slit was located at 2 mm from the plasma so that the high transverse magnification of about 100 facilitates the analysis of the inherent spatial gradients. As for the spectral resolution

($R = 8\,000$), it was achieved by using a PET crystal set up in the Johann geometry and employed at the first order.

Figure 4 shows the evolution of the experimental profile of the Ly_γ line of Al XIII as the spatially-integrated slice Δz increases in thickness from $z = 0$ at the bottom of the crater until including either $z = 14$ μm (solid line) or $z = 20$ μm (dashed line). For all laser shots corresponding to the same conditions, the observed spectra demonstrate the same qualitative features.

Because the spectrograph was inclined, the emission from the entire dense shock-region plasma was accessible, corresponding to the first spatially-integrated slice of $\Delta z = 5$ μm. Between 5 and 15 μm, the spatial integration involved a progressively less dense plasma. For $\Delta z = 14$ μm the profile exhibited two pronounced dips in the *near* red wing. The dips were located at 6 mÅ and 9 mÅ from the center of the line. These experimental positions are in excellent agreement with the theoretical calculations by the code IDEFIX allowing for the electronic shielding: they yielded the X-dip positions to be 6 mÅ and 9 mÅ, respectively, as presented in the previous section. It had been checked by hydro-simulations [28] that the electron densities involved in the spatial integration interval 5 μm–15 μm are consistent with those optimizing the visibility of the dips in the wing.

For a larger thickness of the spatial integration, *i.e.* $\Delta z = 20$ μm, only discontinuities of the slope of the line profile in the *near* red wing were still visible as remnants of the X-dips. In the latter case, the average density for the selected plasma slice was getting too low for observing the X-dips.

We would like to emphasize two facts. First, the observed dips, being located in the *near* wing, correspond to the part of the line profile where the signal-to-noise ratio is still reasonable. Second, they are reproducible in all spectra observed for different Δz [22]. These two features distinguish the observed dips from the jitter in the far wings. The latter corresponds to the experimental noise and its spectral positions are not reproducible in spectra observed for different Δz.

5 Conclusions

We presented a significant advance in the theory of the X-dip phenomenon. This advance was achieved by performing simulations that did not employ the asymptotic assumption (1). They were based on a quasimolecular approach and also allowed for the shielding by electrons. We showed that this advanced theory is in excellent agreement with our experimental results.

We emphasize that this X-dip phenomenon of a *multidisciplinary* character (bringing together atomic physics and plasma physics) should have a significant practical importance. Indeed, further experimental studies of X-dips, using various "radiator-perturber" pairs, would serve for producing not-yet-available fundamental data on CE between multi-charged ions, virtually inaccessible by other experimental methods.

The X-dip phenomenon is also important from the theoretical point of view for the following reasons. Let us compare this phenomenon to Quasimolecular Satellites (QS) observed in spectral lines emitted by laser-produced plasmas [27]. The QS result from extrema in transition energies *unrelated to avoided crossings*. The X-dips and the QS have one thing in common: in the course of a collision, for a relatively short period of time, the electron is shared by two ionic centers – a transient molecule (quasimolecule) is formed. However, other features of the X-dip phenomenon are unique and clearly distinguish it from the QS.

First, for a given pair of multicharged ions, the X-dips are observed in plasmas of densities by two or three orders of magnitude lower than densities, at which the QS are observed. This is because the internuclear distance, corresponding to avoided crossings responsible for the X-dips, is typically by an order of magnitude greater than the internuclear distance, corresponding to extrema in transition energies unrelated to avoided crossings. Coupled with the requirement that, for favorable observation conditions, the mean interionic distance in a plasma should be close to the corresponding internuclear distance of interest, this explains the above dramatic difference in favorable plasma densities. Thus, the X-dips are the only one quasimolecular phenomenon that could be observed at relatively "low" densities of laser-produced plasmas.

Second, it should be emphasized that – in distinction to the X-dips – the QS can be unrelated to CE (despite statements to the contrary in some papers). The mere fact that, for a relatively short time, the electron is shared between two ionic centers does *not* necessarily mean that CE would occur. Indeed, CE requires that the electron, which was initially bound at one ionic center, would finally end up at the other ionic center.

For pairs, consisting of two different ionic centers (*i.e.*, for heteronuclear systems), CE does *not* happen in the process leading to the QS for the following reason. CE would require a coupling of those two quasimolecular terms that asymptotically (at $R \to \infty$) would correspond to the electron being bound by only one or only the other ionic center. If the coupling would be there, then at relatively small R, where these two terms come close together, an avoided crossing would occur. However, in the reality, at the internuclear distance corresponding to an extremum in transition energies, there is no avoided crossing of the terms responsible for the QS and therefore no CE occurs.

For pairs consisting of identical ionic centers (*i.e.*, for homonuclear systems), the fundamental principle of the indistinguishableness of identical particle should be taken into account. Therefore, in this case in a plasma medium at the absence of particle beams, it is impossible to determine that the electron, which was initially bound at one ionic center, finally ended up at the other ionic center. Moreover, if in the course of a collision, only elastic scattering would occur without any CE, QS would be still emitted.

In addition, for homonuclear systems, the internuclear distance $R_{\rm ext}$ corresponding to an extremum in transition energies (*i.e.*, the distance responsible for QS) usually

differs from the effective internuclear distance R_{ce} where CE occurs. Indeed, CE in this case is a resonant process requiring a quasidegeneracy of two energy levels corresponding to symmetric and antisymmetric wave functions. This condition is met at relatively large R, where the energy gap between these two levels is exponentially small. However, at $R \approx R_{ext}$, the energy gap between these two levels becomes significant and dramatically diminishes the probability of CE. Besides, the distance R_{ce} decreases as the relative velocity v_{rel} of the colliding ionic centers increases (see, *e.g.*, [1]), while the distance R_{ext} does not depend on v_{rel}. Therefore, at relatively large velocities v_{rel}, the distance R_{ext} can exceed the distance R_{ce} by an order of magnitude or more. The point is that the effective distance (and therefore, the cross-section) for one process is velocity-dependent, while for another process it is not. This shows once again that the two processes are physically independent of each other: neither one is a prerequisite of the other.

Thus, the bottom line is that the X-dip phenomenon is *the only one signature of CE* in profiles of spectral lines emitted by plasmas. This further enhances the importance of our first experimental observation of the X-dip phenomenon in laser-produced plasmas, as well as the enhancement of the accuracy of the underlying theory that we achieved by using the code IDEFIX. Our experimental study of this phenomenon in laser-produced plasmas containing other "radiator-perturber" pairs is ongoing. A preliminary analysis of the experimental spectra is encouraging; results on the X-dips involving other "radiator-perturber" pairs are expected to be presented elsewhere in the nearest future.

References

1. B.H. Bransden, M.R.C. McDowell, *Charge Exchange and the Theory of Ion-Atom Collisions* (Clarendon Press, Oxford, 1992)
2. F.B. Rosmej, V.S. Lisitsa, Phys. Lett. A **244**, 401 (1998)
3. R.C. Isler, R.E. Olson, Phys. Rev. A **37**, 3399 (1988)
4. S.S. Churilov, L.A. Dorokhin, Yu.V. Sidelnikov, K.N. Koshelev, A. Schulz, Yu.V. Ralchenko, Contrib. Plasma Phys. **40**, 167 (2000)
5. R.C. Elton, *X-Ray Lasers* (Acad. Press, New York, 1990)
6. F.I. Bunkin, V.I. Derzhiev, S.I. Yakovlenko, Sov. J. Quant. Electron. **11**, 981 (1981)
7. A.V. Vinogradov, I.I. Sobelman, Sov. Phys. JETP **36**, 1115 (1973)
8. A. Engel, K.N. Koshelev, Yu.V. Sidelnikov, S.S. Churilov, C. Gavrilescu, R. Lebert, Phys. Rev. E **58**, 7819 (1998)
9. K.N. Koshelev, H.-J. Kunze, Quant. Electron. **27**, 164 (1997)
10. H.-J. Kunze, K.N. Koshelev, S. Steden, D. Uskov, H.T. Wieschebrink, Phys. Lett. A **193**, 183 (1994)
11. K.N. Koshelev, Yu.V. Sidelnikov, S.S. Churilov, L.A. Dorokhin, Phys. Lett. A **191**, 149 (1994)
12. P. Beiersdorfer, R.E. Olson, L. Schweikhard, P. Liebisch, G.V. Brown, J. Crespo Lopez-Urrutia, C.L. Harris, P.A. Neill, S.B. Utter, K. Widmann, in *The Physics of Electronic and Atomic Collisions*, edited by Y. Itikawa (American Institute of Physics, New York, 2000), p. 626
13. I.H. Hutchinson, *Principles of Plasma Diagnostics* (Cambridge Univ. Press, Cambridge, 1987)
14. E. Oks, Phys. Rev. Lett. **85**, 2084 (2000)
15. E. Oks, J. Phys. B At. Mol. Opt. Phys. **33**, 3319 (2000)
16. M. Pieksma, C.C. Havener, Phys. Rev. A **57**, 1892 (1998)
17. W. Fritsch, H.B. Gilbody, R.E. Olson, H. Cederquist, R.K. Janev, K. Katsonis, G.L. Yudin, Phys. Scripta T **37**, 11 (1991)
18. H. Cederquist, A. Barany, Phys. Scripta T **37**, 94 (1991)
19. St. Böddeker, H.-J. Kunze, E. Oks, Phys. Rev. Lett. **75**, 4740 (1995)
20. E. Oks, E. Leboucher-Dalimier, Phys. Rev. E **62**, R3067 (2000)
21. E. Oks, E. Leboucher-Dalimier, J. Phys. B **33**, 3795 (2000)
22. E. Leboucher-Dalimier, E. Oks, E. Dufour, P. Sauvan, P. Angelo, R. Schott, A. Poquerusse, Phys. Rev. E **64**, R065401 (2001)
23. E. Leboucher-Dalimier, P. Sauvan, P. Angelo, A. Poquerusse, R. Schott, E. Dufour, E. Minguez, A. Calisti, J. Quant. Spectrosc. Radiat. Transfer **71**, 493 (2001)
24. E. Leboucher-Dalimier, A. Poquerusse, P. Angelo, Phys. Rev. E **47**, R1467 (1993)
25. E. Leboucher-Dalimier, A. Poquerusse, P. Angelo, I. Gharbi, H. Derfoul, J. Quant. Spectrosc. Radiat. Transfer **51**, 187 (1994)
26. E. Leboucher-Dalimier, P. Angelo, P. Gauthier, P. Sauvan, A. Poquerusse, H. Derfoul, T. Ceccotti, S. Alexiou, T. Shepard, C. Back, E. Foerster, M. Vollbrecht, I. Uschmann, J. Quant. Spectrosc. Radiat. Transfer **58**, 721 (1997)
27. P. Gauthier, S.J. Rose, P. Sauvan, P. Angelo, E. Leboucher-Dalimier, A. Calisti, B. Talin, Phys. Rev. E **58**, 942 (1998)
28. F. Ogando, P. Velarde, J. Quant. Spectrosc. Radiat. Transfer **71**, 541 (2001)